Available online at www.elixirpublishers.com (Elixir International Journal)

Earth Science

Elixir Earth Sci. 87 (2015) 35977-35982

ISSN: 2229-712X

Ground Penetrating Radar Detection of Buried Utilities using Numerical Modeling and Hilbert Transformation: Case Study from Lagos Nigeria

Adepelumi Adekunle Abraham[1,*], Akindulureni John Olaolu[1] and Fayemi Olalekan[2]

[1]Department of Geology, Obafemi Awolowo University, Ile-Ife, Nigeria

[2]Institute of Geology and Geophysics, Chinese Academy of Science, Beijing, China

ARTICLE INFO

Article history:

Received: 18 January 2016;

Received in revised form:

24 July 2016;

Accepted: 29 July 2016;

Keywords

Finite-difference time-domain, GPR,

Perfectly matched layer,

Hilbert transformation,

Instantaneous amplitude

ABSTRACT

The application of finite-difference time-domain (FDTD) numerical modeling and Hilbert transformation for the image enhancement and detection of buried engineering utilities using surface ground-penetrating radar (GPR) technique is demonstrated in a typical sedimentary terrain of Lagos Nigeria. Accurate delineation and precise location of such subsurface features is of effective use for engineering and environmental studies. A traverse magnetic (TM-) mode formulation was adopted for the models; and perfectly matched layer (PML) absorbing boundaries were implemented for wave absorption at the modeling grid edges. Four synthetic models were developed; three single-layer models of a single pipe buried at depth (z) of 2m, two pipes 10m apart and concrete bars buried at z=1.5m, and one double-layered model of multiple pipes buried at z=1.5m. The electrical properties of the models are; single-layered earth-system (vadose zone): $\varepsilon_r = 9$, $\sigma = 1\text{mS/m}$; pipes: $\varepsilon_r = 12$, $\sigma = 1\text{mS/m}$, bars: $\varepsilon_r = 16$, $\sigma = 1\text{mS/m}$. The two-layered subsurface, had a thin-layer of air-earth interface of $\varepsilon_r = 1$ and $\sigma = 0$, upper layer of vadose zone sediment and lower-layer (saturated zone) of $\varepsilon_r = 25$ and $\sigma = 5\text{mS/m}$. The μ was set equal to its free space value, μ_0 for all the materials. The 2D GPR data acquired in some parts of Southwestern Nigeria and processed using basic functions such as dewow, filtering and application of gains. The resulting GPR radargrams were subjected to advanced attribute analysis using Hilbert transformation (HF) in order to establish the suitability of HF for GPR signal image enhancement that would aid the interpretation of the location of the buried utilities. The model investigations revealed that the electrical and the magnetic properties of the medium hosting the buried utilities, and the depth of burial plays a major role in controlling the image resolution obtained in a sedimentary terrain. The results from the field data are in general agreement with the numerical FDTD modeling experiments.

Introduction

Geophysical methods have become very popular and reliable tools for the investigation of subsurface underground features for environmental, engineering, geotechnical applications to mention a few. This is due to their minimally/non-invasive, cost-effective and fast field implementation. In particular, near-surface investigations have been done using a variety of Near-Surface geophysical (NSG) methods including resistivity-imaging techniques, seismic refraction, VLF electromagnetics, Ground-penetrating radar (GPR) etc., for detecting underground pipes and buried infill within sinkholes, landfill investigations, karst studies, subsurface collapse structures, buried and failing foundations, fracture and fault detection, structural and stratigraphic feature detection and site characterization (McDowell, 1975; Sowerbutts, 1988; Adepelumi et al., 2006b; Farooq et al., 2012, Adepelumi et al., 2014).

GPR has become one of the most frequently used non-destructive testing (NDT) because it is a relatively quick technique that gives an overall qualitative continuous internal image of the shallow subsurface. It provides high-resolution imagery of the subsurface, ranging from centimetres to tens of metres in depth and precise horizontal and vertical positioning. It was first put into practice in the 1970's for ice sounding in Antarctica and has since gained wide acceptance. Subsurface imaging for structural/stratigraphic features and buried utilities have become enhanced due to its high spatial resolution of features with a variety of GPR antennas (25MHz - 4GHz) for construction, lithologic, archaeological, geophysical prospecting and engineering purposes.

A general review of GPR background, theory, and implementation considerations as well as a description of various available system approaches and equipment is presented by Daniels et al. (1988). De Beukelaar et al. (2004) demonstrated the application of GPR survey in the investigation of the risk of relocating a buried concrete culvert and the effect in relation to the location and detection of various other known and unknown subsurface objects as cables and pipelines. Loken (2007) successfully used GPR in a variety of highway applications, including detection of air-filled and water-filled voids, locating subsurface vertical cracks, locating subsurface anomalies including buried

Tele:

E-mail addresses: adepelumi@gmail.com

objects, peat deposits, and near-surface bedrock; and analyzing rutting mechanisms. Hebsur et al. (2010) successfully employed the simultaneous use of low and medium frequency (80MHz and 200MHz) GPR data together with sophisticated signal processing techniques such as Hilbert Transform and Support Vector Machines to detect buried concrete footings at a demolished building site. The approach was detected with a high level of accuracy the buried objects that were non-cylindrical in form. Accurate detection of rebar location using GPR proves to be very useful in assessing roadway/bridge deck concrete structure, buried utility detection and subsurface void detection (Hebsur et al., 2012).

Numerical modeling and simulation of GPR systems has become a widely used tool for understanding subsurface scattering mechanisms and propagation of radar-waves. Numerical GPR models provide a means of examining the relationship between subsurface properties and GPR. Various methods have been presented for numerical modeling and simulation of GPR using ray-based methods (Goodman, 1994; Cai and McMechan, 1995), frequency-domain methods (Powers and Olhoeft, 1994; Zeng et al., 1995), integral methods (Ellefsen, 1999), pseudospectral methods (Carcione, 1996; Casper and Kung, 1996, Lui and Fan, 1999) and finite difference time-domain (FDTD) method (Wang and Tripp, 1996; Bourgeois and Smith, 1996; Bergmann et al., 1996; Teixeira et al., 1998; Holliger and Bergman, 2002). However, the FDTD technique, a complex equation-based numerical modeling technique has evolved into the most used and one of the most advanced modeling tools involving arbitrarily complicated inhomogeneities, when sophisticated interpretations and simulation the propagation of the GPR waves in different media are required (Lampe et al., 2003; Jol, 2009). Gürel & Oguz (2000) simulated three-dimensional GPR data using the FDTD method and perfectly-matched layer (PML) absorbing boundary conditions to simulation realistic scenarios using two transmitters and one receiver (TRT configuration) in order to cancel out the direct rays received by the both transmitters at the receiver. The results demonstrated the advantages of using the TRT configuration and various polarizations of the dipole antennas to simulate GPR models. Irving and Knight (2006) developed flexible MATLAB codes for FDTD modeling of 2D-GPR, implementing PML absorbing boundaries applicable to complex modeling of surface and crosshole/vertical radar profiling radar using transverse magnetic (TM-) and transverse electric (TE-) mode formulation respectively. Furthermore, Seyfi and Yaldiz (2012) developed a simulator based on an energy-efficient algorithm using 2D FDTD to scan all regions ranging from an inclined or rough subsurface layer and buried objects.

The main thrust of this paper is to demonstrate the applicability of finite-difference time-domain (FDTD) synthetic modeling and Hilbert transformation for subsurface image detection and enhancement of buried engineering utilities using surface ground-penetrating radar (GPR) technique in a typical sedimentary terrain of Lagos Nigeria that is very often associated with hydrocarbon spillage. Adepelumi et al. (2006a) posited that, environmental pollution due to oil spillage remains a major problem of global environmental concern than was previously the case in sub-Sahara Africa. Of recent, the Nigerian National Petroleum Corporation places the quantity of petroleum spilled into the environment in Nigeria at 2,300 cubic metres with an average of 300 individual spills annually. It is pertinent to note that, most of the hydrocarbon pipelines in Nigeria are laid in sedimentary terrain. These pipelines are often vandalized or corroded due to poor maintenance culture, thus allowing leakage from underground storage tanks (UST) and/or pipelines into the environment and concomitantly polluting the entire ecosystem. Combination of these factors possibly continues to contribute to the menace of oil spillage that often lead to colossal revenue lost to the Government.

Location and geology of the Study Area

The investigated area is located in Southeastern part of Lagos State (Fig. 1). It constitutes part of the Dahomey basin of Nigeria. It is a fast growing metropolitan city with estimated population of fourteen million people. Sedimentation in this basin dates back to early Cretaceous after the separations of African – South America landmasses and subsequent opening of the Atlantic Ocean (Omatsola and Adegoke, 1981). The area lies within the Coastal Plateau geomorphic unit. The surface local geology of the study area is consistent with the regional geological setting of Lagos area as described by Longe, et al., (1987) which consist of Ilaro Formation and the Recent littoral alluvial to Coastal Plain sand deposits (Benin Formation). The Ilaro Formation consists of rather massive sandstone with local clay intercalations. The Ilaro Formation is fine to medium grained, and is fairly well sorted. The The Ilaro Formation lies conformably on the Oshoshun Formation (Lower – Middle Eocene) and locally unconformably beneath the Benin Formation (Oligocene-Pleistocene). The Ilaro Formation is mostly likely to be Middle to Upper Eocene in age. The Benin Formation consists of continental sands with shale intercalations usually with good groundwater potential. The Ilaro Formation is estimated to be about 70 m thick and shows rapid lateral facies changes (Durotoye, 1975). Geologic and geodetic evidences point to the existence of some large faults beneath the area that may possibly suggest the extension of the Romanche and Charcot fracture zones.

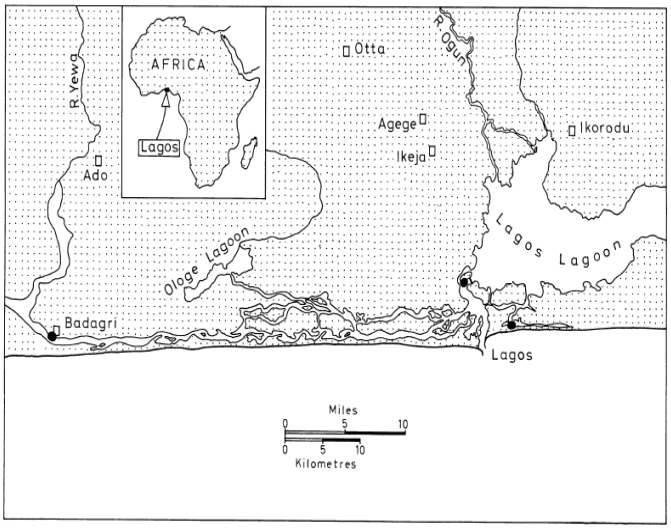

Figure 1. Location Map of the Investigated area in Lagos Nigeria.

Methodology

The FDTD method is a widely known time-domain method used for representing wave propagation (Seyfi and Yaldiz, 2012). It is a simple technique for computational electromagnetics like simulation of GPR data ***using Maxwell's equations and its constitutive equations (Annan, 2005).***

$$\nabla * \mathrm{E} = \mathrm{J} + \frac{\partial \mathrm{B}}{\partial \mathrm{T}} \quad (1)$$

$$\nabla * H = J + \frac{\partial D}{\partial T} \quad (2)$$

$$\nabla * D = \rho \quad (3)$$

$$\nabla * B = 0 \quad (4)$$

$$J = \sigma E \quad (5)$$

$$D = \varepsilon E \quad (6)$$

$$B = \mu H \quad (7)$$

Where E = electric field strength vector, B = magnetic flux density vector, D = dielectric displacement vector, H = magnetic field intensity, ρ = electric charge density, J = electric current density vector, t = time, σ = Electrical conductivity, ε = Dielectric permittivity and μ = Magnetic permeability.

A description of the way the FDTD works is given by Hebsur et al. (2012); the problem geometry of electromagnetics is divided into a spatial grid, where electric and magnetic field components are placed at certain discrete positions in space and it solves the Maxwell's equations in time at discrete time instants which are set conditionally. To solve these equations, first the Maxwell's curl equations are converted to scalar derivatives which are first ordered space and time derivatives. These derivatives are approximated by finite differences and then a set of equations are constructed for the calculation of field values at a future time instant from the values of fields at a past time instant. And hence FDTD constructs the time marching algorithm that simulates the progression of fields in time.

The theory of the FDTD codes used in this work, including the governing analytical equations, their finite-difference approximations, numerical stability and dispersion criteria, and boundary conditions are explained in Irving and Knight (2006). The formulation was implemented in the MATLAB environment for the generation of models and display of results. The models included single and multiple buried pipes and concrete bars, and the synthetic data obtained could be used to improve understanding of the spatial changes in properties of subsurface utilities scanned by GPR waves. Although the algorithm does not incorporate certain features like dispersion in electrical properties, it captures many crucial aspects of GPR surveying and has a significantly lower run-time compared to more elaborate algorithms.

The modeling codes were developed based on Maxwell's curl equations in the frequency domain;

$$\nabla \times E = -i\omega\mu H \quad (8)$$

$$\nabla \times H = \sigma E + i\omega\varepsilon E \quad (9)$$

where $i = \sqrt{-1}$, ω = angular frequency and E, H, σ, ε and μ maintain their respective definitions. The general case of a complex stretched coordinate space is assumed for the implementation of the PML absorbing boundaries (Chew and Weedon, 1994; Gedney, 1998). The PML approach chosen offers superior attenuation of reflections from edges, requires only small number of cells to be effective, is well suited to parallel implementations and is independent of the properties of the media being modeled (Gedney, 1998; Roden and Gedney, 2000)

Field GPR data was collected using a Geophysical Survey System Incorporated SIR system-2000 equipment in continuous collection mode. The survey was carried out using a 200MHz monostatic antenna with the antenna oriented parallel to the survey direction (Parallel-Broadside). ASTM D6432-11 (2011) Standard Guide for Using the Surface Ground Penetrating Radar Method for subsurface investigation was adopted. The GPR data were acquired over surfaces with known buried utilities and features. The antenna was preset with three gain points in order to improve the scans during data acquisition while thirty-three (33) scans per meter were taken (representing 3 cm station spacing) with a sampling window of 300ns with offset of +25 ns. A 16-fold stack was used for the traces during data recording to improve the signal to noise (S/N) ratio of the data. The GPR data positioning was calibrated using a survey wheel (odometer) and each radar trace contains 1024 points per trace. Basic processing steps were applied to the radargrams, such as time-zero correction, background removal, dewow (removal of low-frequency noise), band-pass filtering (to remove unwanted high-frequency components) and application of gains (Figure 2).

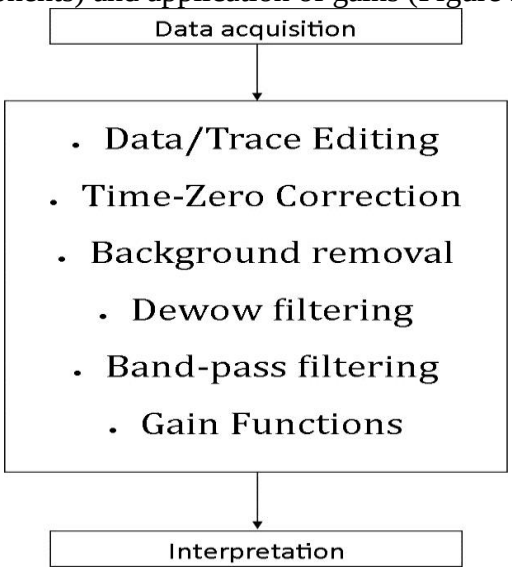

Figure 2. Processing sequence for the 2D monostatic GPR data

The concept of Hilbert Transform (HT) was introduced by Papoulis (1962). However, their application to geophysical data analysis was first tested by Červený and Zahradník (1975). The early worker showed that from Hilbert spectral of a signal, the non-stationary and nonlinear nature of the signal can be revealed (Huang and Wu, 2008). The application of HT as a signal processing tool in ground penetrating radar (GPR) was introduced by Gao et al. (1997), and it gained wide acceptance after it was confirm by several researchers working on seismic data processing and complex seismic trace analysis among which is Luo et al (2003) where that showed that a signal $x(t)$ and its HT $\hat{x}(t)$ have the following properties: the same amplitude spectrum, the same autocorrelation function, that a signal $x(t)$ and its HT $\hat{x}(t)$ are orthogonal, and that the HT of $\hat{x}(t)$ is $-x(t)$. Thus, the HT has become a classic technique for estimating instantaneous parameters from GPR data. This approach extends a real signal to an analytical signal, by converting the input GPR signal to both its real and imaginary components, and subsequently extracting the instantaneous parameters from the newly derived analytical signal. Gao et al. (2014) applied the HT method in mapping underground pipelines in a suburb of China. In the publication, they showed that the image obtained from the GPR data processed using HT produce subsurface images that closely resembled the shape and size of the buried pipelines. In this work, Instantaneous amplitude functions of the Hilbert transformation were applied to the processed GPR data to enhance the interpretability of the buried utilities and

subsurface structures in the radar images obtained (Kim et al. 2007; Adepelumi et al, 2013).

Results and Discussion

Synthetic Models

Synthetic models were developed for the analysis of the dipole antenna pair located above a lossy homogeneous/inhomogeneous material half space where the subsurface features are located and the propagation of the Electric and Magnetic field components of the GPR waves. In such configuration, the transmit element of the radar unit emits an electromagnetic pulse that propagates into the ground, where it interacts with the target. This interaction results in a diffracted electromagnetic field which is measured by the receiver element of the radar. By changing the location of the radar on the soil interface and recording the output of the receive antenna as function of time (or frequency) and radar location, one obtains the scattering data, which can be processed to get an image of the subsurface. Three scenarios are depicted within a single-layer model; a single pipe buried at z=2m depth, two pipes 10m apart and concrete bars buried at z=1.5m. The single-layered earth-system has electrical properties $\varepsilon_r = 9$ and $\sigma = 1\text{mS/m}$ and the features occur at depth in the subsurface within the vadose zone. The pipes have $\varepsilon_r = 12$ and $\sigma = 1\text{mS/m}$ while the bars have $\varepsilon_r = 16$ and $\sigma = 1\text{mS/m}$ The source and receiver were placed on the air-earth interface and gradually moved along the traverse in the region of the buried utilities. For all the materials, μ was set equal to its free space value, μ_0. Another scenario of a two-layered subsurface, with a thin-layer of air-earth interface of $\varepsilon_r = 1$ and $\sigma = 0$ is depicted for multiple pipes; the upper layer of vadose zone sediment has $\varepsilon_r = 9$ and $\sigma = 1\text{mS/m}$ and the lower-layer, representative of materials within the saturated zone has $\varepsilon_r = 25$ and $\sigma = 5\text{mS/m}$ (Figure 3). The models and their corresponding electrical properties used for developing them are shown in Figure 4. The source pulse had a dominant frequency of 200 MHz. Figure 5 show snapshots of the Ey field component at various times during the FDTD simulation for the source located at position x=10m. Because of the PML absorbing boundaries implemented, no reflections can be seen coming from the edges of the modeling domain in any of the panels. At later times, we capture the wavefield as it is spreading outwards from the source before and after it has encountered any heterogeneity within the earth.

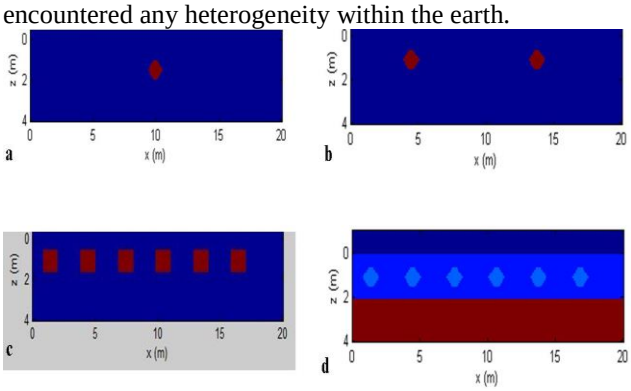

Figure 3: Single- and double-layered earth systems generated for the FDTD numerical modeling with buried utilities.

(a) single pipe buried at z=2m (b) two pipes separated by 10m at z=1.5m (c) multiple buried bars at z=1.5m (d) multiple pipes buried within the vadose zone at z=1.5m

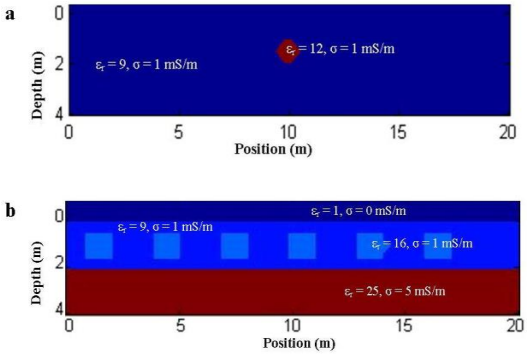

Figure 3. Single- and double-layered earth systems generated for the FDTD numerical modeling with buried utilities. (a) single pipe buried at z=2m (b) two pipes separated by 10m at z=1.5m (c) multiple buried bars at z=1.5m (d) multiple pipes buried within the vadose zone at z=1.5m

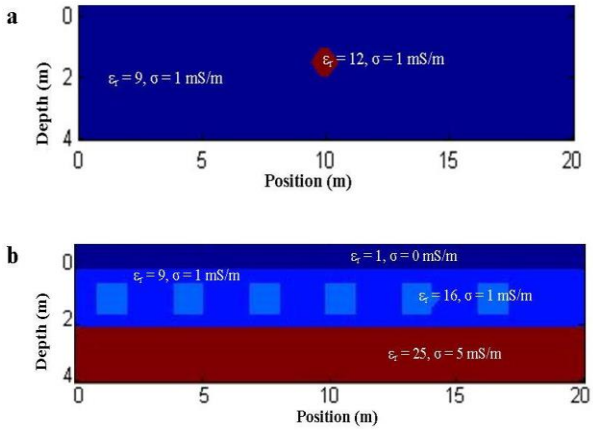

Figure 4. Material electrical properties used for the models for the (a) pipe and single earth-layered system (b) metal bars and double-earth layered system with thin-layered air-earth interface

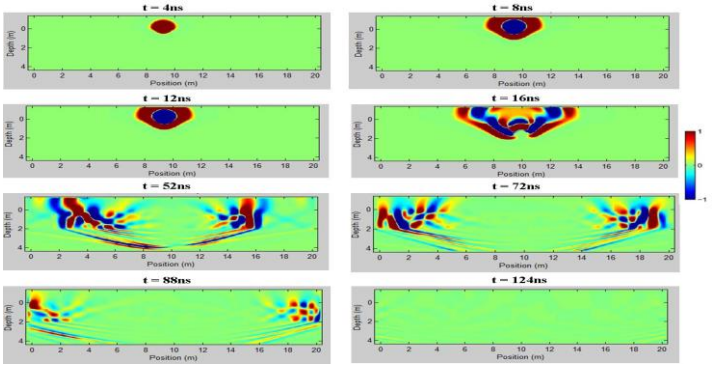

Figure 5. Snapshots showing amplitude of Ey wavefield at different times during TM-mode FDTD modeling. Source is located at x=10m, z=0m

At source position x=0, t=4ns, the source pulse is strongest and just begins to propagate into the subsurface. The wavefield continues to spread through t=12ns to 104ns when it starts to disperse and become attenuated. The wavefield is suppressed at t=240ns and becomes completely attenuated. At source position x=10m, t=4ns, we capture the wavefield as it is spreading outwards from the source before it has encountered any heterogeneities in the subsurface. At t=16ns, the wavefield has clearly encountered the buried pipe(s) in the subsurface layer and is being partly reflected to the surface. At

t=52ns, the energy reflected from the pipe has reached the air-earth interface. Although the earth model developed is a simple single-layered system, the propagating wavefield becomes complicated rather quickly. The maximum frequency contained in source pulse = 283.2031MHz and the minimum wavelength in simulation grid = 0.21172 m. The synthetic radargrams obtained for the buried pipe models depict the diffraction hyperbola of the pipes within the single-layer medium (Figure 6). Linear events in the image are the direct air and ground arrivals and the propagation of the EM wavefield through the earth model delineates the pipes at their accurate positions of burial and giving the hyperbolic reflections at the top of the pipes in the vadose zone layer. The synthetic GPR image for the concrete bars and multiple bars are shown in Figure 7. Linear events in the section are as a result of direct air and ground arrivals and reflections from the boundary of vadose and saturated zones. The layer boundary is visible, although it does not extend fully to both ends of the GPR section because of time shifts caused by the velocity of the anomalies in the upper layer.

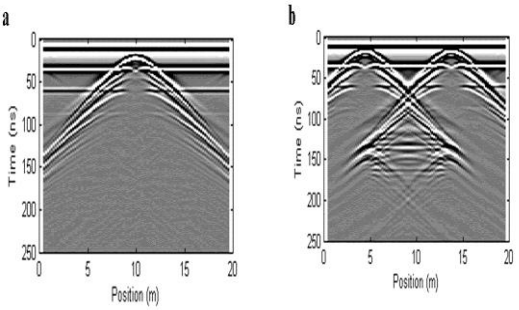

Figure 6.Synthetic radargrams for the (a) single pipe (b) two pipes separated by 10 m

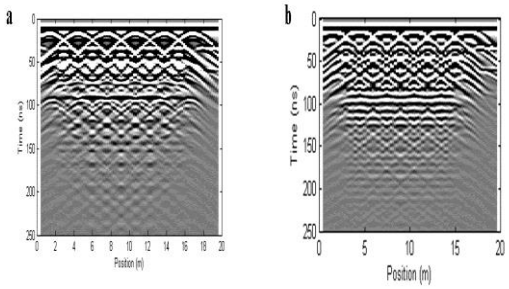

Figure 7. Synthetic radargrams for the (a) multiple pipes (b) multiple bars

Hilbert Transformation

For further understanding of the reflection signatures of utilities within the subsurface, GPR lines were acquired over positions of known buried features and a bridge deck in southwestern Nigeria. The acquired GPR data radargram were processed using basic steps (time-zero correction, background removal, dewow, band-pass filtering and application of gains). The processed radar images of the buried pipe, road culvert, metal rebars and bridge deck are shown in Figure 8. Advanced processing of the radargrams using attribute analysis was done by applying the Hilbert transformation functions to the data.

This approach extends a real signal to an analytical signal, by doing the HT for the real signal to get its imaginary counterpart, and extracts the instantaneous parameters by comparing the imaginary part and the real part of the analytical signal (Liu & Oristaglio, 1998).

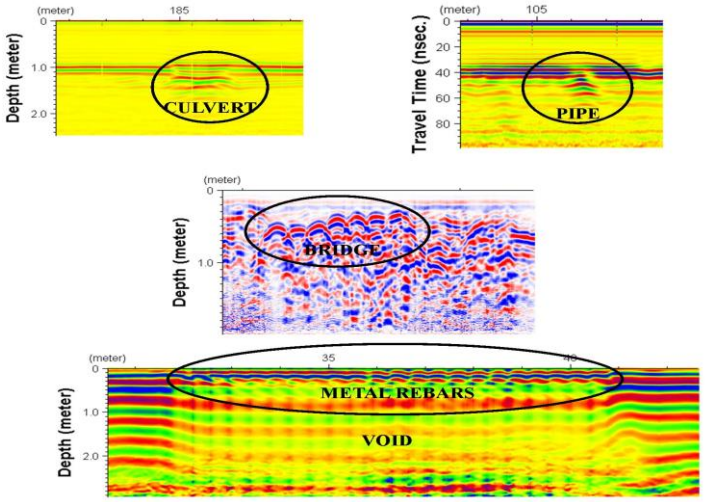

Figure 8. Processed GPR sections showing the culvert, pipe, metal rebar and subsurface void

GPR attributes have been used to delineate subsurface and geologic targets and to define critical fluid and rock properties and the interpretation of GPR data is usually done by examining the radar amplitude, phase, and frequency in radar sections. Therefore, these three simple attributes – amplitude, phase and frequency are the fundamental procedures for geological and subsurface structural interpretation in GPR attribute analysis (Le Van Quyen et al., 2001). The attribute analysis was done using the Instantaneous amplitude attribute on the radargrams. Envelope (instantaneous amplitude) calculates the absolute value of each wavelet by converting negative wavelets to positive wavelets, resulting in a positive mono pulse wavelet. This process is used to emphasize the true resolution of the data, and can be used to simplify data and evaluate the signal strength and reflectivity. The benefit of the envelope display is that it reflects the resolution of the data. It is possible to get a false sense of resolution because of the oscillatory nature of the radar pulse as the bandwidth or envelope of the pulse is what determines resolution, and not the time between zero crossings (which reflects the dominate frequency in the data). To this end, the envelope is extremely useful for depicting the spatial resolution of the data (Dojack, 2012). The envelope display of the radargrams is presented in Figure 9.

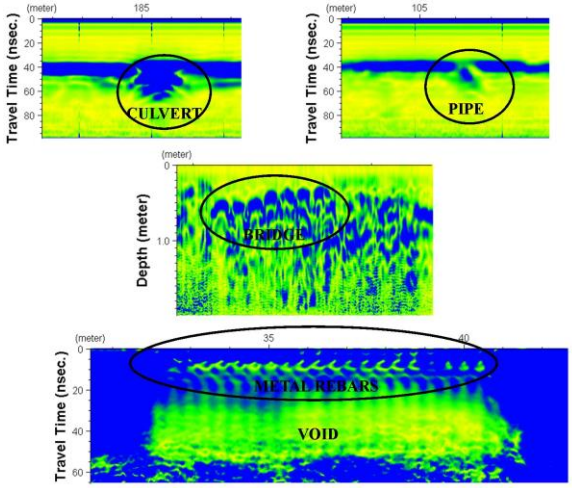

Figure9.Envelope (Instantaneous amplitude) sections showing the enhanced images of the culvert, pipe, metal rebar and subsurface void

Conclusion

The applicability of the finite-difference time-domain

(FDTD) modeling technique constrained byperfectly matched layer absorbing boundary conditions to eliminate wave scattering at grid edges and mapping engineering utilities such as pipes/pipelines, rebar and voids found in a typical sedimentary environment of have been shown through this study. Further, the roles that electrical and magnetic properties of the host medium (soil) would play in the detection of the various buried utilities have been successfully tested in this work. The practical relevance of the advanced signal processing method called Hilbert transformation to ground penetrating radar (GPR) subsurface imaging processing have been established The synthetic radar radargrams obtained from the FDTD modeling experiment carried out in this study are consistent with the GPR signal responses obtained where the utilities were buried. The usefulness of the Hilbert transformation in improving the resolution of the processed GPR sections have been pointed, and should be incorporated into conventional routine GPR data processing.

References

Adepelumi, A. A; A. A. Solanke; O. B. Sanusi; A. M. Shallangwa (2006a) Model tank electrical resistivity characterization of LNAPL migration in a clayey-sand formation Environmental Geology. Vol. 50, 1221-1233

Adepelumi A, Yi MJ, Kim JH, Ako BD, Son JS (2006b) Integration of surface geophysical methods for fracture detection in crystalline bedrocks of south-western Nigeria Hydrogeology Journal 14, 1284-1306.

Adepelumi A. A., Akindulureni J. O., Agih C. O., Olubodun B. B. & Evinemi I. E. (2014): Peat stratigraphy mapping using ground penetrating radar and geotechnical engineering implications.International Journal of Advanced Geosciences, 2 (2), 86-96

Adepelumi AA, Fayemi O & Akindulureni J (2013) Geophysical Mapping of Subsurface Stratigraphy beneath a River Bed Using Ground Penetrating Radar: Lagos Nigeria Case Study. Universal Journal of Geoscience 1, 1, 10-19.

Annan, A. P. (2005): Ground Penetrating Radar. In: Near-Surface Geophysics, Dwain K. Butler (Editor), Investigations in Geophysics No. 13, pp. 357 – 434.

ASTM D6432-11 (2011) Standard Guide for Using the Surface Ground Penetrating Radar Method for subsurface investigation. 1 - 18.

Bergmann, T., Robertsson, J.O.A., Holliger, K., (1996). Numerical properties of staggered finite-difference solutions of Maxwell's equations for ground-penetrating radar modeling. Geophysical Research Letters 23, 45–48.

Bourgeois, J.M., Smith, G.S., (1996). A fully three-dimensional simulation of a ground-penetrating radar: FDTD theory compared with experiment. IEEE Transactions on Geoscience and Remote Sensing 34, 36–44

Cai, J., McMechan, G.A., (1995). Ray-based synthesis of bistatic ground-penetrating radar profiles. Geophysics 60, 87–96

Carcione, J.M., (1996). Ground-penetrating radar: wave theory and numerical simulation in lossy anisotropic media. Geophysics 61, 1664–1677.

Casper, D.A., Kung, K.S., (1996). Simulation of ground-penetrating radar waves in a 2-D soil model. Geophysics 61, 1034–1049

Červený, V and Zahradník, J (1975) Hilbert transform and its geophysical applications. Acta Universitatis Carolinae. Mathematica et Physica, Vol. 16 (1975), No. 1, pp. 67-81.

Chew, W.C., Weedon, W.H., 1994. A 3-D perfectly matched medium from modified Maxwell's equations with stretched coordinates. IEEE Microwave and Optical Technology Letters 7, 599–604.

Daniels, D. J. Gunton, D. J. and Scott. H. F. (1988) Introduction to subsurface radar. IEE Proceedings, Part F: Communications , Radar And Signal Processing, 135-f, August 1988.

DE BEUKELAAR. P, DIJKSTRA.J, MEINSTER, M and WILMS, P (2004). Locating a buried culvert and the detection of underground cables and pipelines using GPR. Near Surface 2004 - 6-9 September 2004. 10th European Meeting of Environmental and Engineering Geophysics, Utrecht, The Netherlands.

Durotoye, A. B. (1975). Quaternary sediments in Nigeria (C.A. Kogbe edited). Geology of Nigeria, Elisabeth Press, Lagos, pp.431-451.

Ellefsen, K.J., (1999). Effects of layered sediments on the guided wave in crosswell radar data. Geophysics 64, 1698–1707

Gao, J., W. Wang, and G. Zhu (1997) Wavelet transform and signal instantaneous characteristics, Acta Geophysica Sinica, Vol. 40, xxx.

Goodman, D., (1994). Ground-penetrating radar simulation in engineering and archeology. Geophysics 59, 224–232.

Hebsur, A, Muniappan, N, Rao, E. P and Venkatachalam, G. (2010). A Methodology for Detecting Buried Solids in Second-use Sites Using GPR. Indian Geotechnical Conference – 2010, GEOtrendz. 49-52

Hebsur, A. V. Muniappan, N. Rao, E. P. Venkatachalam G. (2012). 14th International Conference on Ground Penetrating Radar (GPR) June 4-8, 2012, Shanghai, China @ ISBN 978-1-4673-2663-6

Holliger, K and Bergman, T (2002) Numerical modeling of borehole georadar data, Geophysics, Vol. 67, pp. 1249-1257,

Huang, N. E and Wu, Z (2008) A review on Hilbert-Huang transform: Method and its applications to geophysical studies. Reviews of Geophysics, 46 (2), pp. 1 – 23.

Irving J & Knight R (2006) Numerical modeling of ground penetrating radar in 2-D using MATLAB. Computers and Geosciences, 32, 1247-1258.

Jol HM. Ground Penetrating Radar: Theory and Applications. Elsevier Science; 2009.

Kim, J. H., Cho, S. J. and Yi, M. J. (2007) Removal of ringing noise in GPR data by signal processing: Geosciences Journal, v. 11, no. 1, pp. 75 – 81.

Dojack, L. (2012) Ground Penetrating Radar Theory, Data Collection, Processing, and Interpretation: A Guide for Archaeologists. 2012

Lampe B, Holliger K, Green A. G. (2003) A finite-difference time-domain simulation tool for ground-penetrating radar antennas. Geophysics, 2003; 68:971 -987.

Le Van Quyen M, Foucher J, Lachaux J-P, Rodriguez E, Lutz A, Martinerie J and Varela F. (2001) Comparison of Hilbert transform and wavelet methods for the analysis of neuronal synchrony. J. Neurosci. Meth, vol. 111: pp. 83-98.

Levent Gürel, and Ugur Oguz (2000). Three-Dimensional FDTD Modeling of a Ground-Penetrating Radar. IEEE TRANSACTIONS ON GEOSCIENCE AND REMOTE SENSING, VOL. 38, NO. 4, JULY 2000. 1513-1521

Levent SEYFI and Ercan YALDIZ (2012). Turk J Elec Eng & Comp Sci, Vol.20, No.3.

Liu Lambo and Oristaglio Michael (1998) GPR SIGNAL ANALYSIS: INSTANTANEOUS PARAMETER ESTIMATION USING THE WAVELET TRANSFORM.

Proceedings of the 7th International Conference on Ground Penetrating Radar. 219-224

Loken, M. C. (2007). Use of ground penetrating radar to evaluate Minnesota roads. Research Rep. No. MN/RC-2007-01, Minnesota Dept. of Transportation, St. Paul, Minn.

Longe, E.O., Malomo, S., and Olorunniwo, M.A., (1987). Hydrogeology of Lagos metropolis, Journal of African Earth Sciences, 6, 3, 163-174.

Lui, Q.H., Fan, G., (1999). Simulations of GPR in dispersive media using a frequency-dependent PSTD algorithm. IEEE Transactions on Geoscience and Remote Sensing 37, 2317–2324.

Luo, Y; Dossary, S. A and Marhoon, M (2003). Generalized Hilbert transform and its applications in geophysics. The Leading Edge, pp. 198-202.Gao, L; Liu, H and Yu, X (2014). Study on the image recognition of pipeline based on ground penetrating radar. Ejge, Vol. 19, pp. 439-445.

McDowell, P.W. (1975). Detection of clay filled sink-holes in the chalk by geophysical methods. Quarterly Journal of Engineering Geology, 8:303-310.

Muhammad Farooq, Samgyu Park, Young Soo Song, Jung Ho Kim, Mohammad Tariq and Adepelumi Adekunle Abraham (2012). Subsurface cavity detection in a karst environment using electrical resistivity (er): a case study from yongweol-ri, South Korea. Earth Sci Res SJ Vol 16, No 1, 75 – 82.

Omatsola, M.E and Adegoke, O.S (1981). Tectonic Evolution and Cretaceous Stratigraphy of Dahomey Basin. Journal of Mining and Geology, 18 (1), pp.130-137,

Papoulis, A (1962). Hilbert Transforms. The Fourier Integral and Its Applications. New York: McGraw-Hill, pp. 198-201, 1962.

Powers, M.H., Olhoeft, G.R., (1994). Modeling dispersive groundpenetrating radar data. Proceedings of the 5th International Conference on Ground-Penetrating Radar, Waterloo, Ontario, pp. 173–183.

Roden, J., Gedney, S., (2000). Convolution PML (CPML): an efficient FDTD implementation of the CFS-PML for arbitrary media. IEEE Microwave and Optical Technology Letters 27, 334–339.

Sowerbutts, W.T.C. (1988). The use of geophysical methods to locate joints in underground metal pipelines. Quarterly Journal of Engineering Geology, 21:273-281.

Teixeira, F. L, Chew, W. C, Straka, M, Oristaglio, M. L and Wang, T (1998) Finite-difference time-domain simulation of ground penetrating radar on dispersive, inhomogeneous and conductive soils IEEE Transactions on Geoscience and Remote Sensing, Vol. 36, pp. 1928-1936.

Wang, T., Tripp, A.C., (1996). FDTD simulation of EM wave propagation in 3-D media. Geophysics 61, 110–120.

Zeng, X., McMechan, G.A., Cai, J., Chen, H.W., (1995). Comparison of ray and Fourier methods for modeling monostatic ground-penetrating radar profiles. Geophysics 60, 1727–1734.